VNU Journal of Science: Natural Sciences and Technology, Vol. 39, No. 4 (2023) 35-45

VNU Journal of Science: Natural Sciences and Technology

Journal homepage: https://js.vnu.edu.vn/NST

Original Article

Unleashing Potential: First Vietnamese 3D *in vitro* Model Using Induced Pluripotent Stem Cell-Derived Cardiomyocytes

Dang Thi Minh Anh[1], Nguyen Xuan Hung[2,*]

[1]*VNU University of Science, 334 Nguyen Trai, Thanh Xuan, Hanoi, Vietnam*

[2]*Vinmec Hi-Tech Center, 458 Minh Khai, Hai Ba Trung, Hanoi, Vietnam*

Received 26 July 2023
Revised 28 September 2023; Accepted 24 October 2023

Abstract: Advancements in studying cardiovascular diseases (CVDs) face challenges related to cell sources and utilizing animal models. To mitigate these limitations, three-dimensional (3D) *in vitro* modeling using human induced pluripotent stem cell-derived cardiomyocytes (iCMs) has emerged as a promising approach. In this study, human induced pluripotent stem cells (hiPSCs) were successfully differentiated into cardiomyocytes and subsequently used to generate spheroids via the hanging drop method. We comprehensively characterized the formation, fusion, and beating capability of the generated spheroids. The hiPSCs were efficiently differentiated into cardiomyocytes, exhibiting contractile activity and expressing cardiac-specific markers such as α-actinin and cardiac troponin. Subsequent results demonstrated the successful formation of iCM-derived cardiac spheroids within 48 hours, with beating activity observed after two days cultured in an ultra-low attachment 96-well plate. In addition, similar to the iCM monolayer, the established spheroids also positively expressed α-actinin. Notably, the spheroids exhibited rapid assembly and maintained survival and stable beating throughout the observation period. These findings highlight the potential of establishing a robust *in vitro* iCM-derived 3D spheroids model for drug testing and cardiovascular disease modeling, typically for Vietnamese people.

Keywords: 3D, cardiomyocytes, induced pluripotent stem cells, *in vitro*, disease model, spheroid.

1. Introduction

Cardiovascular diseases (CVDs) remain the leading cause of global mortality, responsible for approximately 17.9 million deaths annually [1]. CVDs encompass a range of heart and blood vessel disorders, including coronary heart disease, cerebrovascular disease, and rheumatic heart disease [1]. In Vietnam, CVDs also pose a significant health burden, ranking among the primary causes of death. According to data from the World Health Organization (WHO), CVDs accounted for 31% of all deaths in Vietnam in 2016, resulting in over 170,000 fatalities [2]. Given this alarming prevalence, the study of cardiovascular diseases holds significant urgency and importance. These studies allow for unraveling the intricate

* Corresponding author.
E-mail address: v.hungnx1@vinmec.com

https://doi.org/10.25073/2588-1140/vnunst.5581

mechanisms underlying these diseases, shedding light on their etiology while also contributing to developing effective pharmacological interventions targeting CVDs.

Animal models, particularly mice, have been crucial in advancing our understanding of cardiac pathogenic mechanisms [3]. However, there are significant disparities between murine and human hearts, including differences in ion channel roles, calcium handling, cardiomyocyte development, and cardiac electrophysiological properties. These disparities pose challenges in creating accurate models for human diseases and contribute to the limited success of translating treatments from murine preclinical studies to human clinical trials [4].

In terms of *in vitro* modeling, the current *in vitro* models based on monolayer cell cultures have limitations. Cells grown in a single layer on a flat surface lack a 3D structure that closely mimics the *in vivo* environment [5]. In contrast, 3D culture systems offer a more accurate representation of *in vivo* cellular structure and microenvironment, thus improving the reliability of *in vitro* testing [6]. Cardiomyocytes (CMs) cultured in a 3D environment exhibit enhanced physiological relevance, as they retain their contractile properties and display prolonged viability compared to monolayer cultures [7].

Human primary cell lines have emerged as a crucial tool for *in vitro* investigations of cardiac diseases, offering advantages over animal models. Utilizing human cardiomyocytes helps circumvent the aforementioned challenges associated with interspecies differences, providing a more accurate representation of human cardiac pathophysiology. However, the limited availability of primary cardiomyocytes has fueled interest in utilizing cardiomyocytes derived from human induced pluripotent stem cells as an alternative cell source for modeling the human heart. hiPSC-derived cardiomyocytes offer several distinct advantages, including their potential application in disease modeling, toxicity studies, drug discovery, and regenerative therapy [8, 9]. These versatile cells are promising in advancing our understanding of cardiac diseases and developing novel therapeutic approaches.

In contrast to conventional cell types, iPSCs represent a unique reflection of an individual's genotype, as they are derived from the patient's somatic cells, such as erythroid progenitors [10], umbilical cord blood hematopoietic stem cells [11], or fibroblasts [12]. This intrinsic origin endows iPSCs with significant relevance for personalized medicine and genetic investigations. iPSCs can be differentiated into diverse cell lineages, including CMs [13, 14] and cardiac fibroblasts [14], among others. This capacity is harnessed in developing patient- and disease-specific models, which offer unparalleled multidimensional insights into individual conditions and provide a platform for assessing novel therapeutic interventions [15]. Patients carrying known disease-related mutations play a crucial role in shaping disease-specific iPSC lines, making significant strides in our ability to model various conditions [15]. For instance, pioneering iPSC-derived cellular models were established for disorders like LEOPARD syndrome [16], long QT syndrome [17], and hypertrophic cardiomyopathy (HCM) [18]. Additionally, channelopathies resulting from specific cardiac ion channel mutations can be effectively replicated using iPSC-CMs [15]. The quality of these disease models hinges on how iPSC-CMs manifest disease phenotypes that mirror their physiological counterparts [15]. For instance, iPSC-CMs generated from individuals carrying HCM-related mutations in the myofilament myosin heavy chain 7 (MYH7) faithfully exhibit phenotypic traits such as abnormal calcium handling, increased myofibril content, and cellular hypertrophy at baseline and upon stress [18]. Furthermore, disease models constructed using iPSCs serve as invaluable tools for emulating the physiological response of patients to various drugs. This capability enables us to rigorously assess the efficacy and safety of medications before administering them [15]. For example, iPSC-CMs derived from patients with dilated cardiomyopathy (DCM) closely mimic patient

responses to β agonists and β blockers, providing a valuable platform for pre-treatment drug evaluation [15]. Such patient-specific iPSC models hold tremendous promise in advancing our understanding of diseases and improving treatment strategies.

In Vietnam, animal cell-based models have been the primary approach in cardiovascular disease research and drug development [19-21]. However, a recent breakthrough in generating Vietnamese hiPSCs has provided a solid foundation for our investigations [10, 11]. This showcase demonstrates the potential of hiPSC technology and serves as a driving force propelling our research endeavors in cardiovascular diseases. Recognizing the critical importance of cardiovascular disease research and the transformative possibilities offered by harnessing 3D *in vitro* modeling techniques with hiPSC-derived cardiomyocytes, our goal was to develop a fully characterized cardiac spheroid derived from iCMs. The outcomes presented in this study aim to lay the groundwork for establishing robust 3D *in vitro* models, paving the way for in-depth investigations into cardiomyopathies, particularly in drug discovery and therapeutic development tailored to the Vietnamese population.

2. Materials and Methods

2.1. Materials

The main reagents and instruments used in this study were: hiPSC line (Vinmec Hi-Tech Center), StemMACS™ CardioDiff Kit XF (Miltenyi, USA), mTeSR1 medium (StemCELL, Canada), MEMalpha (Gibco, USA), Trypan Blue Solution (Gibco, USA), Fetal bovine serum (FBS) (Invitrogen, USA), Phosphate-buffered saline (PBS) 1X (Gibco, USA), PolyHEMA (Thermo Fisher, USA), Ethanol 70% (Vinh Phuc Health Corp., Vietnam), Trypsin-EDTA (Gibco, USA), TrypLE (Thermo Fisher, USA), Anti-human Cardiac Troponin T Fluorescein isothiocyanate (FITC) (Miltenyi, USA), Anti-human α-actinin FITC (Miltenyi, USA), Hoechst 33342 (Thermo Fisher, USA), Propidium Iodide (Thermo Fisher, USA), 15 mL centrifuge tube (Corning, USA), 35mm petri dish (SPL, Korea), 1.5 mL eppendorf tube (Eppendorf, USA), ultra-low attachment 96-well plate (Corning, USA).

2.2. Methods

2.2.1. Preparation of HiPSC-derived Cardiomyocytes

Generation of iCMs

Human induced pluripotent stem cell (hiPSC) lines obtained from Vinmec Hi-Tech Center were maintained in 6-well plates using mTeSR1 medium. When hiPSCs reached 60-80% confluence, they were dissociated with TrypLE and collected as single cells. These cells were seeded onto 24-well plates at an appropriate density to initiate differentiation. The differentiation of iPSCs into cardiomyocytes (iCMs) was carried out by sequentially changing the differentiation media according to the instructions provided with the differentiation kit. The beating ability of the differentiated cardiomyocytes was recorded on day 6 of differentiation. On day 12, the cells were subcultured, and after two days, they were transferred to a lactate medium for purification. After three days of purification, the medium was replaced by the MEMalpha + 10% FBS medium. Following an additional 2-3 days of culture in the maintenance medium, the cells were ready to generate spheroids.

iCMs characterization

Cardiomyocytes were initially confirmed by their contractile capability observed on day 6 of differentiation and their distinctive morphological structure throughout the differentiation process. To ensure precise verification, on day 17 of differentiation, cardiomyocytes underwent immunofluorescence staining utilizing specific markers: actinin, cardiac troponin, and four′, 6-diamidino-2-phenylindole (DAPI). Actinin and cardiac troponin are particular markers for cardiomyocytes, whereas DAPI staining shows cell nuclei. In detail, cells cultured on matrigel-coated wells were washed with PBS and then fixed with 4% paraformaldehyde in PBS for 15 minutes. They were subsequently permeabilized with 0.3% Triton-X100 in PBS for 3 minutes

and incubated for 30 minutes with 3% bovine serum albumin (BSA) in PBS at room temperature. The cells were then incubated overnight with antibodies at 4 °C, and DAPI was added to visualize the nuclei. Finally, EVOS M7000 Microscope Imaging System was utilized to capture images for analysis.

2.2.2. Generation of iCM Spheroids

iCMs were rinsed with PBS 1X. To detach cells, 0.05% Trypsin-EDTA was added and incubated at 37 °C for 5 minutes. The trypsinization was then stopped by adding MEMalpha + 10% FBS medium. The cells were transferred to a 15 mL centrifuge tube and centrifuged at 300 g for 4 minutes. Subsequently, cell counting was performed using a hemocytometer with trypan blue solution (1:1 ratio of cell stock to trypan blue). The supernatant was discarded, and the cells were resuspended at the appropriate concentration. Two distinct cell concentrations of 30,000 cells/spheroid and 60,000 cells/spheroid were employed to assess the influence of initial cell concentration on spheroid characteristics.

For the formation of spheroids, 35 mm Petri dishes were used. The bottom of the dish was filled with PBS 1X to prevent the drops from evaporating. The dish lid was inverted, and 20 µL of cell suspension was gently deposited onto the bottom of the lid. Drops were placed sufficiently apart to avoid contact. The inverted lid was then placed onto the bottom of the dish, which was filled with 1X PBS. The entire setup was incubated at 37 °C with 5% CO_2. Spheroids formed within approximately 48-72 hours.

2.2.3. Long-term Culture of iCM Spheroids

Preparation of non-adherent plates

The ultra-low attachment 96-well plate was coated with polyHEMA (2-hydroxyethyl methacrylate) dissolved in ethanol to prevent spheroid attachment. Each well was filled with 30 µL polyHEMA solution and left to evaporate under ultraviolet light (UV) exposure without the lid inside a sterile hood. Once dried, the plate was ready to receive spheroids.

Transfer spheroids after formation

After iCM 3D spheroids formed over time, they were transferred from the lid of the culture dish to the 96-well plate coated with polyHEMA. The medium was changed every two days.

2.2.4. Characterization of Spheroids

To assess the characteristics of the generated spheroids, we evaluated the spheroid for its size, beating activity, fusion capability, and the presence of iCM-specific markers.

Spheroid size

To evaluate the relationship between input cell concentration and spheroid size, the size of the formed cardiac spheroids was monitored over time using images captured with an inverted microscope. ImageJ software was employed for measuring the spheroid size.

Spheroid fusion ability

Two spheroids were transferred to the same well after being stably cultured on an ultra-low attachment 96-well plate for two days to evaluate the fusion ability. The extent of fusion between the spheroids was observed using images acquired with an inverted microscope.

Beating ability

The beating capacity of the spheroids was continuously monitored and recorded throughout the experimental period.

Fluorescence staining

The immunofluorescence staining was performed in spheroids similarly to that in 2D culture, with some modifications. Specifically, fixation was extended to 1 hour, and permeabilization was carried out overnight a 4 °C. The blocking step lasted 2 hours, and washing was performed multiple times at each step. The antibody incubation was performed similarly to 2D iCMs.

Moreover, double-staining with Propidium Iodide (PI) and Hoechst was carried out for 1 hour at room temperature. The images were taken by confocal microscopy.

3. Results and Discussion

3.1. Differentiation of HiPSCs into Cardiomyocytes

The hiPSC line obtained from Vinmec Hi-Tech Center was cultured in mTeSR1 medium. Once the cell confluence reached

60-80% (Figure 1), the cells were harvested and initiated the differentiation process into cardiomyocytes. By day 6 of differentiation, the iCMs exhibited spontaneous beating activity (Supplementary Video 1) and displayed distinct morphological changes (Figure 2A). The differentiation process continued until day 12, after which the cells underwent purification to enhance the percentage of cardiomyocytes, following our in-house established protocol. On day 17 of the differentiation process, following the purification of iCMs, immunofluorescent staining was performed using specific markers for cardiomyocytes: α-actinin and cardiac troponin (Figure 3). α-actinin expression served as a distinctive feature, representing the visual appearance of cardiomyocytes, and also provided valuable insights into the arrangement and structure of sarcomeres within these cells. Additionally, cardiac troponin (cTnT) is a specific protein marker exclusive to cardiomyocytes, which plays a crucial role in cellular muscle contraction. The positive expression of cTnT confirmed the presence of cardiomyocytes and offered valuable information about their relative structural characteristics and shapes. The purified iCMs were then stably cultured and prepared for spheroid formation (Figure 2B).

3.2. Generation of Cardiac Spheroid

Establishing a robust 3D *in vitro* model relies on successfully generating cardiac spheroids with desired characteristics. Once the iCMs reached the appropriate stage, they were collected and utilized for spheroid formation using the hanging drop method. This study evaluated two cell concentrations of 30 x 10^3 and 60 x 10^3 cells per drop. The resulting spheroids were assessed based on their formation time, size, and spontaneous beating ability.

We successfully generated cardiac spheroids, which required at least 48 hours to attain sufficient strength for transfer to an ultra-low attachment 96-well plate (data not shown). Following spheroid formation, the structural morphology was monitored over time (Figure 4).

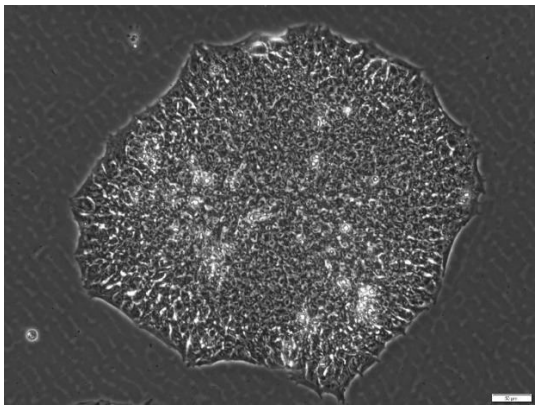

Figure 1. Morphology of hiPSCs. The hiPSCs were cultured in mTeSR1 medium until they reached a confluence of 60-80%, indicating that they had reached the desired standard for initiating the differentiation process. (Scale bar: 50 µm).

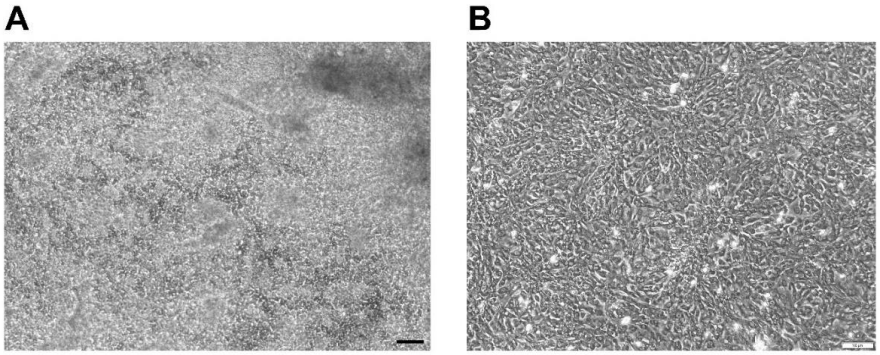

Figure 2. Morphology of hiPSC-derived cardiomyocytes. (A) iCM morphology on day 6 of differentiation, scale bar: 50 µm; (B) iCM morphology before being used for spheroid formation, scale bar: 100 µm.

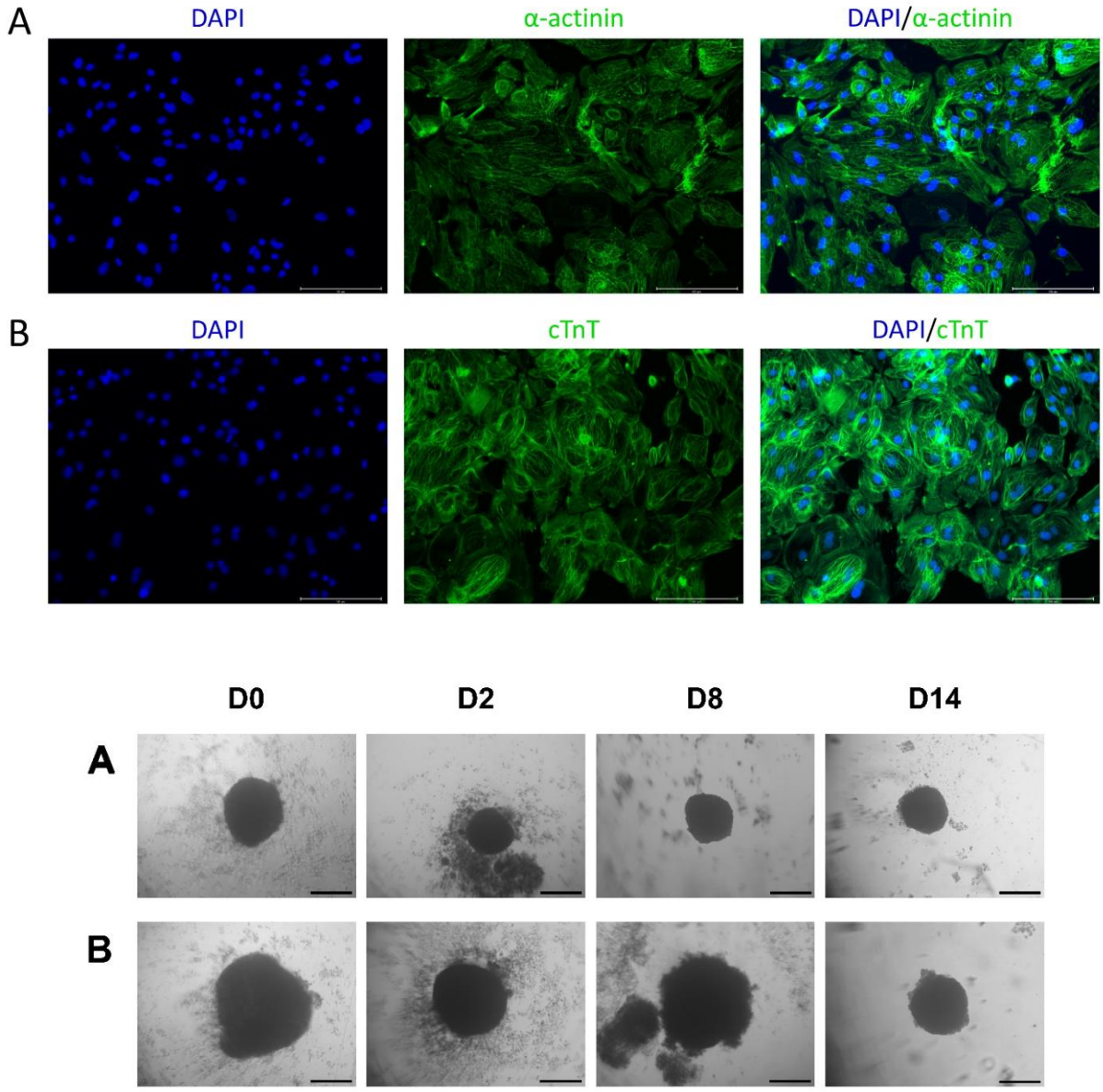

Figure 4. The morphology of cardiac spheroids was observed at four-time points, day 0 (D0), day 2 (D2), day 8 (D8), and day 14 (D14), following their transfer from the lid of a 35 mm petri dish to a polyHEMA-coated ultra-low attachment 96-well plate. (A) The spheroid consisted of 30 x 10^3 cells per spheroid; (B) The spheroid consisted of a concentration of 60 x 10^3 cells per spheroid. (Scale bar: 500 µm).

Analysis of the spheroid size at the time of transfer (D0) revealed an average diameter of 718±33 µm and 1295±13 µm for spheroids generated from a density of 30 x 10^3 and 60 x 10^3 cells per spheroid, respectively. Over time, image analysis demonstrated a gradual decrease in spheroid size, indicating a trend toward enhanced stability. This observation can be attributed to the initial lack of cohesiveness in the spheroids at the time of transfer, resulting

in larger sizes. However, with prolonged culture, the cells within the spheroid became more closely interconnected, leading to a more stable structure and subsequent decrease in size during the early stages, followed by higher stability (Figure 5).

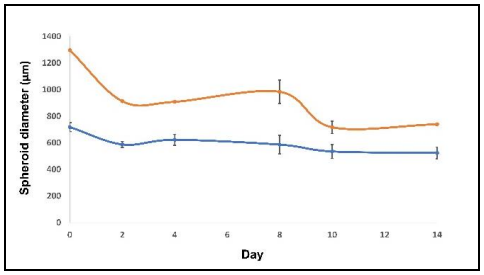

Figure 5. The size changes of spheroids over time. The blue and orange lines represent the spheroid generated from drops containing 30 x 10^3 and 60 x 10^3 cells, respectively.

While the findings of this study demonstrated a relatively stable structure of the established spheroids, similar to the observations made by Polochuk et al., [7], it is essential to note that the spheroids composed solely of iCMs exhibited a less compact structure with a surface that lacks smoothness and tends to deviate from a spherical shape. Regarding the spheroid size, the results show a difference in the average spheroid diameter compared to those reported by Mattapally et al., [22]. Despite using equivalent cell densities, our study yielded a larger sphere size. This discrepancy may be attributed to experimental methods and equipment variations across the studies. Consequently, our plans involve replicating the experiment with a broader range of cell density assessments to gather robust data on the relationship between sphere size and input cell density. This effort aims to contribute to the advancement of disease models and facilitate future research endeavors.

The fusion capacity of spheroids is a crucial criterion for evaluating the quality of the established spheroids. We found that the formed spheroids exhibited a favorable and relatively rapid fusion process, with nearly complete merging observed after two days of aggregation. However, analysis of subsequent images on days eight and 12 revealed that the spheroids still display suboptimal sphericity (Figure 6).

Regarding contractile activity, the spheroids exhibited beating behavior two days after formation (Supplementary Video 2) and remained robust even after fusion. After two days, a relatively uniform beating pattern was observed in the spheroids, corresponding to the fusion level (Supplementary Video 3). Although this beating activity was observed earlier than the findings reported by Mattapally et al., [22], it is essential to note that the two studies employed different methodologies.

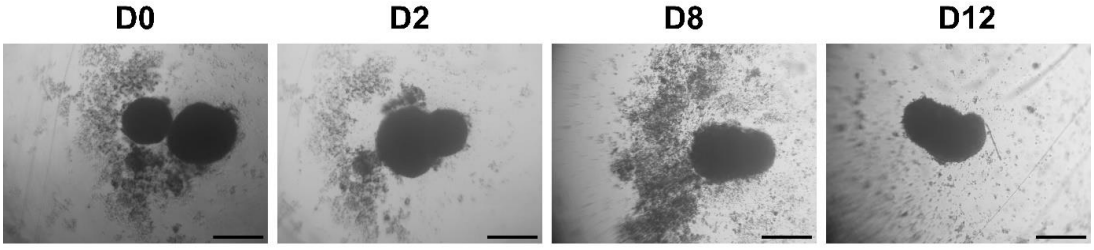

Figure 6. The fusion of spheroids at four-time points, day 0 (D0), day 2 (D2), day 8 (D8), and day 12 (D12). On D0, two spheroids were transferred to the same well, and their fusion was monitored over time. (Scale bar: 500 µm).

To confirm the presence of iCMs within the 3D spheroid model, immunofluorescence staining was performed using a cardiac-specific marker, α-actinin. We revealed a predominant presence of iCMs within the spheroid, characterized by highly positive expression of

α-actinin (Figure 7A). Although the background signal was very high due to the nature of the 3D spheroid containing a dense distribution of iCMs throughout the spheroid, we observed the appearance of the sarcomere structure at the outer edge of the spheroid at high magnification (Figure 7B).

Furthermore, we assessed the viability of the cardiac spheroid at 14-day post-culture by co-staining them with PI (indicative of dead cells) and Hoechst (labeling all cells). Most of the cells in the spheroid were alive, although some dead cells were present (Figure 8).

Besides, the PI signal was not found to be too clear in the center of the spheroid, combined with the stable beating ability (data not shown), suggesting that the spheroid cultured for 14 days still maintained a healthy state without the presence of a necrotic-like core.

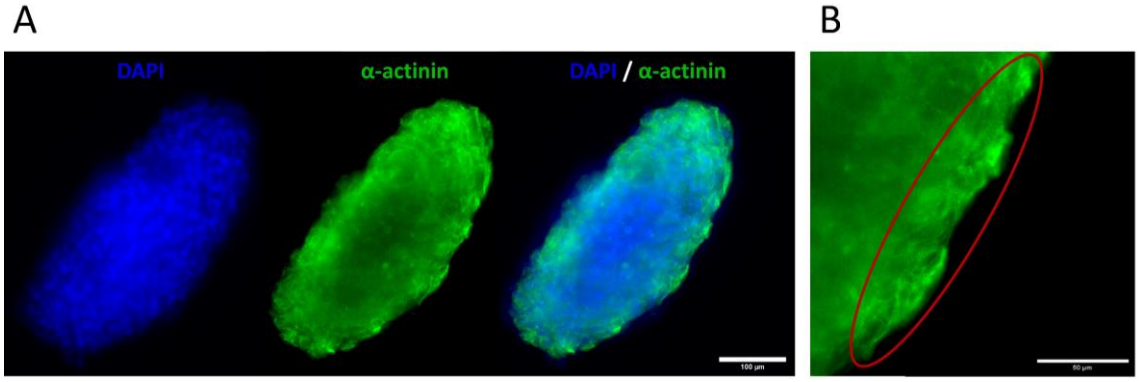

Figure 7. Expression of α-actinin in the cardiac spheroid. (A) Immunofluorescence analysis for α-actinin in the cardiac spheroid after being transferred to a polyHEMA-coated ultra-low attachment 96-well plate. Scale bar: 100 µm. (B) Magnified image showing positive expression of α-actinin in the spheroid. The red circle highlighted the typical sarcomere structure of cardiomyocytes. Scale bar: 50 µm.

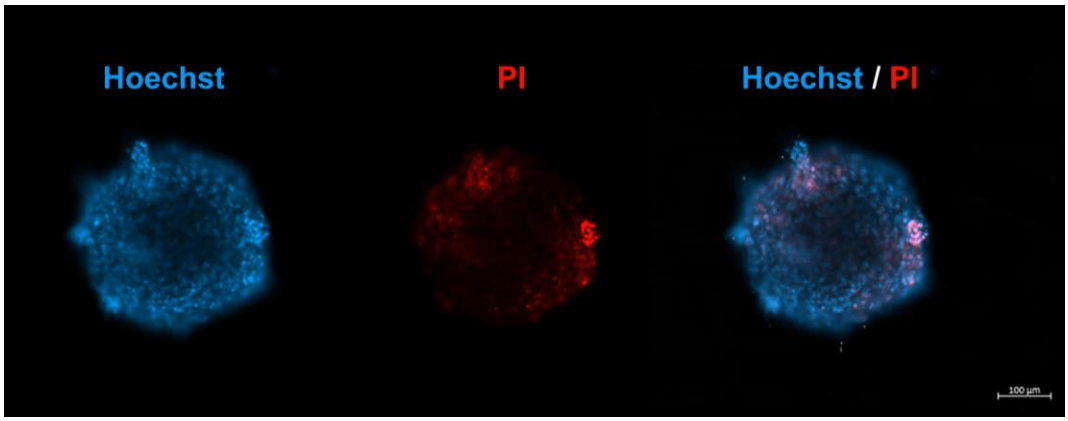

Figure 8. Expression of PI and Hoechst in the cardiac spheroid. Double staining with PI and Hoechst in the cardiac spheroid after 14 days since being transferred to a polyHEMA-coated ultra-low attachment 96-well plate. Scale bar: 100 µm.

4. Conclusion

We successfully differentiated human induced pluripotent stem cells (hiPSCs) into cardiomyocytes, culminating in the formation of robust cardiac spheroids. These spheroids exhibited remarkable attributes, including well-constructed structure, rapid aggregation, and sustained beating ability over an extended duration. These findings offer considerable potential for developing a valuable 3D *in vitro*

model explicitly tailored to investigate the Vietnamese population's cardiovascular diseases. The application of such a model holds promise for advancing drug discovery and facilitating future drug trials, ultimately contributing to improved therapeutic interventions.

Acknowledgements

The authors thank Vinmec Hi-Tech Center for their assistance with the hiPSCs source. This study was funded by the Vietnam National Foundation for Science and Technology Development (NAFOSTED) No.108.06-2018.309 and the project KLEPT.22.01.

References

[1] WHO, Cardiovascular Diseases, https://www.who.int/health-topics/cardiovascular-diseases/, 2023 (accessed on: July 12th, 2023).

[2] WHO, Cardiovascular Diseases in Vietnam, https://www.who.int/vietnam/vi/health-topics/cardiovascular-disease/, 2023 (accessed on: July 12th, 2023).

[3] J. M. J. T. Nerbonne, Studying Cardiac Arrhythmias in the Mouse - a Reasonable Model for Probing Mechanisms?, Trends in Cardiovascular Medicine, Vol. 14, No. 3, 2004, pp. 83-93.

[4] C. Sacchetto et al., Modeling Cardiovascular Diseases with hiPSC-Derived Cardiomyocytes in 2D and 3D Cultures, Int J Mol Sci, Vol. 21, No. 9, 2020, pp. 3404, https://doi.org/10.3390/ijms21093404.

[5] L. Polonchuk et al., Towards Engineering Heart Tissues from Bioprinted Cardiac Spheroids, Biofabrication, Vol. 13, No. 4, 2021, pp. 045009, https://doi.org/10.1088/1758-5090/ac14ca.

[6] P. Sharma et al., Considerations for the Bioengineering of Advanced Cardiac in Vitro Models of Myocardial Infarction, Small, Vol. 17, No. 15, 2021, p. 2003765, https://doi.org/10.1002/smll.202003765.

[7] L. Polonchuk et al., Cardiac Spheroids as Promising in Vitro Models to Study the Human Heart Microenvironment, Scientific Reports, Vol. 7, No. 1, 2017, pp. 7005.

[8] C. W. Van Den Berg et al., Differentiation of Human Pluripotent Stem Cells to Cardiomyocytes under Defined Conditions, Methods Mol Biol, 2016, pp. 163-180, https://doi.org/10.1007/7651_2014_178.

[9] A. S. Smith et al., Human iPSC-Derived Cardiomyocytes and Tissue Engineering Strategies for Disease Modeling and Drug Screening, Biotechnol Adv, Vol. 35, No. 1, 2017, pp. 77-94, https://doi.org/10.1016/j.biotechadv.2016.12.002.

[10] T. H. Nhung Nguyen et al., Generation of an Erythroid Progenitor-Derived iPSC Line, VRISGI002-A, from a Healthy 27-Year-Old Vietnamese Donor under a Feeder-Free System, Stem Cell Res, Vol. 62, 2022, pp. 102824, https://doi.org/10.1016/j.scr.2022.102824.

[11] T. T. Tran et al., Establishment of a Vietnamese Ethnicity Induced Pluripotent Stem Cell Line (VRISGI001-A) from Umbilical Cord Blood Hematopoietic Stem Cells under a Feeder-Free System, Stem Cell Res, Vol. 53, 2021, pp. 102345, https://doi.org/10.1016/j.scr.2021.102345.

[12] R. C. Vinuelas et al., Generation and Characterization of Human Induced Pluripotent Stem Cells (iPSCs) from Hand Osteoarthritis Patient-Derived Fibroblasts, Sci Rep, Vol. 10, No. 1, 2020, pp. 4272, https://doi.org/10.1038/s41598-020-61071-6.

[13] X. Wu et al., A Non-Coding Gwas Variant Impacts Anthracycline-Induced Cardiotoxic Phenotypes in Human iPSC-Derived Cardiomyocytes, Nat Commun, Vol. 13, No. 1, 2022, pp. 7171, https://doi.org/10.1038/s41467-022-34917-y.

[14] J. Yang et al., Phenotypic Variability in iPSC-Induced Cardiomyocytes and Cardiac Fibroblasts Carrying Diverse Lmna Mutations, Front Physiol, Vol. 12, 2021, pp. 778982, https://doi.org/10.3389/fphys.2021.778982.

[15] E. Tzatzalos et al., Engineered Heart Tissues and Induced Pluripotent Stem Cells: Macro- and Microstructures for Disease Modeling, Drug Screening, and Translational Studies, Adv Drug Deliv Rev, Vol. 96, 2016, pp. 234-244, https://doi.org/10.1016/j.addr.2015.09.010.

[16] X. C. Vergara et al., Patient-Specific Induced Pluripotent Stem-Cell-Derived Models of Leopard Syndrome, Nature, Vol. 465, No. 7299, 2010, pp. 808-12, https://doi.org/10.1038/nature09005.

[17] A. Moretti et al., Patient-Specific Induced Pluripotent Stem-Cell Models for Long-QT Syndrome, N Engl J Med, Vol. 363, No. 15, 2010, pp. 1397-409, https://doi.org/10.1056/NEJMoa0908679.

[18] F. Lan et al., Abnormal Calcium Handling Properties Underlie Familial Hypertrophic Cardiomyopathy Pathology in Patient-Specific Induced Pluripotent Stem Cells, Cell Stem Cell, Vol. 12, No. 1, 2013, pp. 101-13, https://doi.org/10.1016/j.stem.2012.10.010.

[19] V. T. Thu et al., Majonoside-R2 Extracted from Vietnamese Ginseng Protects H9C2 Cells against Hypoxia/Reoxygenation Injury Via Modulating Mitochondrial Function and Biogenesis, Bioorg Med Chem Lett, Vol. 36, 2021, pp. 127814, https://doi.org/10.1016/j.bmcl.2021.127814.

[20] T. T. Vu, T. T. Phuong, Hesperidin Extracted from Citrus Reticulata Blanco Protects Cardiac Mitochondria against Hypoxia/Reoxygenation Injury, VNU Journal of Science: Natural Sciences and Technology, Vol. 37, No. 4, 2021, https://doi.org/10.25073/2588-1140/vnunst.5328.

[21] T. B. Pham, T. T. Vu, Cobalt Chloride Alters Mitochondrial Function of in Vitro Cultured Cardiomyocytes in a Dose-Dependent Manner, VNU Journal of Science: Natural Sciences and Technology, Vol. 37, No. 3, 2021, https://doi.org/10.25073/2588-1140/vnunst.5295.

[22] S. Mattapally et al., Spheroids of Cardiomyocytes Derived from Human-Induced Pluripotent Stem Cells Improve Recovery from Myocardial Injury in Mice, Am J Physiol Heart Circ Physiol, Vol. 315, No. 2, 2018, pp. H327-H339, https://doi.org/10.1152/ajpheart.00688.2017.

Supplementary information

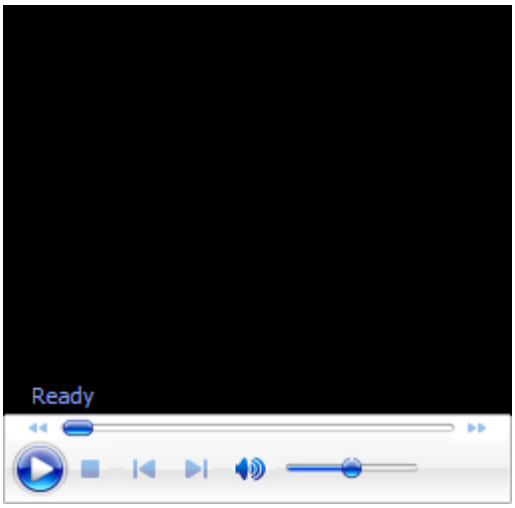

Supplementary Video 1. The spontaneous beating activity was observed on day 6 of the hiPSC-derived cardiomyocyte differentiation. (https://drive.google.com/file/d/1U8-ul90MAQbsf7smTy-K0O2u78PBTxx3/view?usp=sharing).

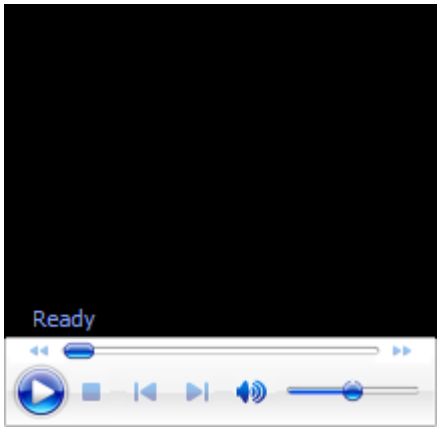

Supplementary Video 2. The beating behavior of iCM-spheroid two days after formation. (https://drive.google.com/file/d/1kEkbGfDu6ZUN99w-_S-WRbxAAz6mSXrR/view?usp=sharing).

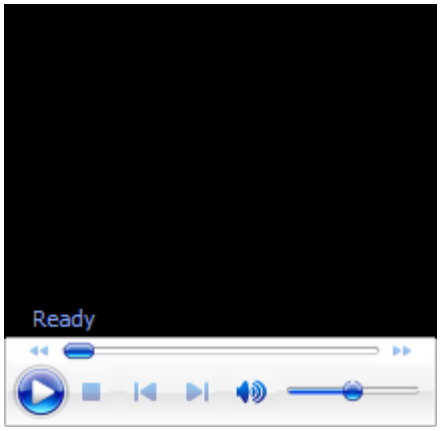

Supplementary Video 3. The beating behavior of two iCM-spheroids on day 2 of fusion progress. (https://drive.google.com/file/d/17VvA_zatwcMsXhzjF1kKC2zkMNIFbL7X/view?usp=sharing).